JOURNAL OF APPLIED ELECTROCHEMISTRY 12 (1982) 241–251

Optimal design of packed bed cells for high conversion

G. KREYSA

Dechema-Institut, Theodor-Heuss-Allee 25, 6000 Frankfurt/M. 97, Federal Republic of Germany

C. REYNVAAN

Deutsche Carbone AG, Talstraße 112, 6000 Frankfurt/M. 56, Federal Republic of Germany

Received 20 July 1981

In connection with the electrochemical purification of metal containing waste waters, the realization of a high concentration decrease per pass is one of the goals of design optimization. For a packed bed cell with crossed current and electrolyte flow directions high conversion in conjunction with a large space time yield requires limiting current conditions for the whole electrode. For establishing the concentration profiles in the direction of flow a plug flow model is used. These considerations result in a new packed bed electrode geometry for which an analytical bed depth function is derived. The basic engineering equations of such packed bed electrodes are given, and design equations for different arrangements are developed. The reliability of this scaling-up method is shown by comparison of theoretically predicted and experimental performance data of two cells. Engineering aspects such as easy matching of cells to waste water properties and parametric sensitivity are discussed. Some technical applications are reported.

1. Introduction

In recent years increasing efforts have been made on the development of electrochemical processes for metal ion removal from waste water. Since at small concentrations the current density is limited by diffusion, only electrode systems which provide a large specific electrode surface work in an economic way. Consequently, three-dimensional electrode systems such as packed bed cells [1–5], fluidized bed cells [6–10], and cells of the 'swiss roll type' [11–15] are suggested and have been tested in the laboratory.

In laboratory investigations, the packed and fluidized bed cell configurations which have been characterized have parallel current and electrolyte flow [3, 16, 17]. In such arrangements, flow length is limited by the penetration depth of the current [17] and a scale-up of the volumetric flow rate can be achieved only by an increase in the cross-section. More convenient ways of scaling-up are provided by crossed current and electrolyte flow directions. In this way, continuous industrial processes can be realized and large containers for circulating liquors can be avoided.

Based on this concept, a new metal containing waste water purification process was developed which allows the metal concentration to decrease with each pass by a factor of 100 or 1000. Specific flow rates of about $10\,h^{-1}$ (volumetric flow rate/cell volume) are achieved compared to those of competing processes such as ion-exchange. A flow diagram of this packed bed electrolysis process is shown in Fig. 1; an extended description has already been published elsewhere [5]. To obtain a high degree of conversion per pass (up to 0.999) a new packed bed electrode geometry was employed. It is the purpose of the present paper to report on the theoretical background of this new cell design. Also, some simple design equations are derived and discussed.

2. Basic equations

In general the description of a three-dimensional electrode with crossed current and electrolyte flow directions requires an extention of the model of Alkire and Ng [18] for a concentric cylinder geometry. Based on the one-dimensional model of a three-dimensional electrode [17] Equations 1 to

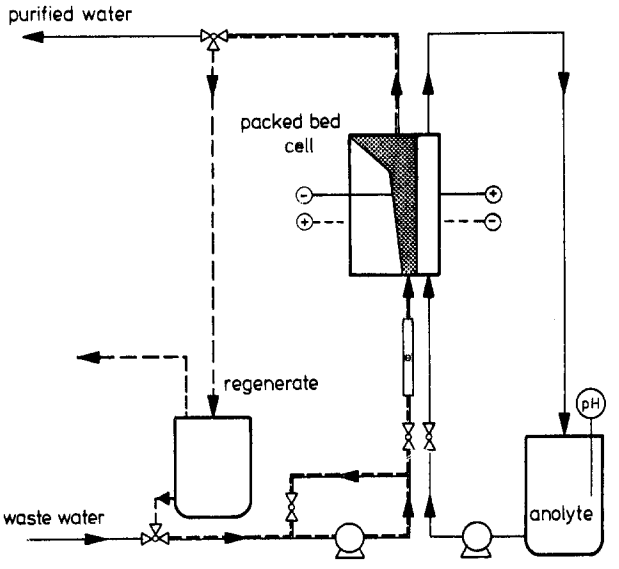

Fig. 1. Flow diagram of the packed bed electrolysis waste water purification process.

3 may be derived for a cubic packed bed electrode (pbe).

$$\frac{d^2\phi_s}{dx^2} = -A_s \frac{i[\eta(x)]}{\chi_s v} \tag{1}$$

$$\frac{d^2\phi_p}{dx^2} = A_s \frac{i[\eta(x)]}{\chi_p(1-v)} \tag{2}$$

$$\frac{d\phi_s}{dx}\chi_s v + \frac{d\phi_p}{dx}\chi_p(1-v) = i_b \tag{3}$$

Using the coordinate definitions of Fig. 2, assuming $\chi_p \to \infty$ characterizing the packed bed situation of the electrode, and applying the ideal tube reactor model [19] yields the following differential equation system.

Ohm's law:

$$\frac{d^2\phi_s}{dx^2} = -A_s \frac{i[\eta(x,y)]}{\chi_s v} \tag{4}$$

charge balance:

$$\frac{d\phi_s}{dx}\chi_s v + A_s \int i[\eta(x,y)]\,dx = i_b(y) \tag{5}$$

ideal tube reactor equation:

$$\frac{dc(x,y)}{dy} = -A_s \frac{i[\eta(x,y)]}{u(y)zF}. \tag{6}$$

This is not really a two-dimensional model but the one-dimensional approach in the x-direction is applied for each possible y as a first-order approximation. For the effective conductivity of the solution, in accordance with Fleischmann [20], only a porosity and no tortuosity correction was made. As a further simplification the bed voidage was assumed to be site-independent. Equation 5 corresponds to Equation 3 but was re-written to be applicable for $\chi_p \to \infty$ also. Radial dispersion is left out in Equation 6. On the one hand, sharp concentration profiles in the x-direction can be obtained for a situation where the current density is varying with x [21]. This indicates a negligible radial dispersion. On the other hand we consider situations where c is independent of x as explained below.

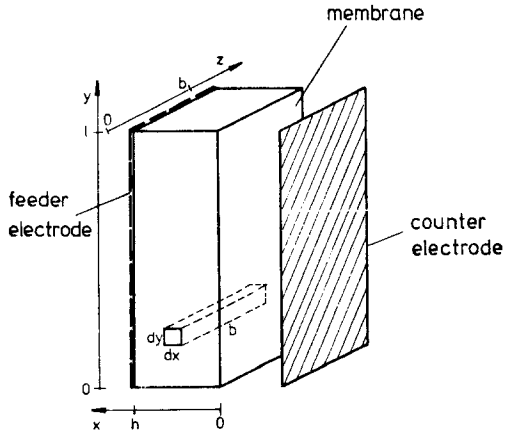

Fig. 2. Coordinates for the three-dimensional electrodes.

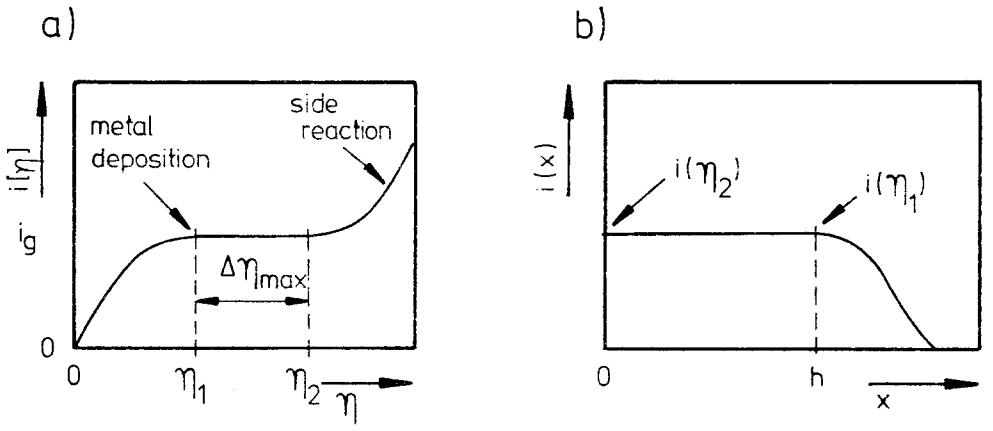

Fig. 3. (a) Microkinetic current density potential curve, (b) resulting current density distribution.

Not all current density distributions, $i\,[\eta(x,y)]$, yield a maximum performance of the pbe. An optimum approach, however, can be gained by the following consideration. The minimum capital costs per m^3 waste water result if a maximum waste water related space time yield (m^3 waste water per h and 1 cell volume) of the electrolysis cell is met. By Faraday's law the space time yield of the pbe can be calculated

$$y_{ST}^{E} = \frac{A_s \bar{i} \beta}{\Delta c z F} \tag{7}$$

which is related to cell space time yield by the equation

$$y_{ST}^{C} = y_{ST}^{E} \frac{1}{1 + V_A/V_B}. \tag{8}$$

Δc is the concentration decrease (moles m^{-3}) which should be achieved by the purification process. As one can see from Equation 8 at a given volume of the anode compartment a maximum cell space time yield requires a maximum electrode yield, and a maximum possible bed volume which is restricted by the current density distribution within the electrode. Equation 7, assuming a diffusion controlled metal deposition (see Fig. 3a), shows the maximum electrode yield requires a maximum possible value of the mean current density. This demand is met if, at each point of the electrode, the full limiting current density corresponding to the local concentration is realized.

$$i[\eta(x,y)] = i_g[c(y)]. \tag{9}$$

The same condition results if, for a given cell length, a maximum degree of conversion is required and radial dispersion is low or negligible. This is important especially in waste water purification applications. If at each point limiting current conditions are used and the plug flow model is applied, then $dc(x,y)/dy$ in Equation 6 is independent of x. This also means that c and i are functions of y only, as indicated by the right hand term of Equation 9. A larger current density should be avoided since otherwise the current efficiency becomes less. Assumption of such an optimum current density distribution means that the overpotential variation ranges from η_1 near the feeder electrode to η_2 near the membrane as depicted in Fig. 3. In practical cases of scaling-up it may be advantageous to underestimate somewhat this maximum possible potential difference $\Delta\eta$ to ensure the validity of Equation 9. For the situation given by Equation 9 at each y the optimum bed depth $h(y)$ can be calculated in the same way as previously shown [17]. If one considers c varying with y and dp, and k as a function of y, one obtains

$$h(y) = \left[\frac{v d_p(y) \chi \Delta\eta \beta}{3(1-v) z_i c_i(y) F k(y)}\right]^{0.5} \tag{10}$$

From Equation 10 the resulting basic geometry of the pbe cells will be considered below. For a constant particle diameter, $d_p(y)$, the bed depth along the flow length, y, of the electrode increases corresponding to the concentration decrease within the cell. β is the current efficiency related to species i if more than one electroactive species is present in the electrolyte. If c_e^t is the total equi-

valent concentration, then

$$\beta = \frac{z_i c_i}{c_e^t} \tag{11}$$

The mass transfer coefficient can be calculated by the dimensionless correlation [22]:

$$\frac{vk(y)d_p(y)}{(1-v)D} = 0.6\left(\frac{\nu}{D}\right)^{0.33}\left(\frac{u(y)d_p(y)}{(1-v)\nu}\right)^{0.5} \tag{12}$$

which can be summarized as

$$k(y) = k'u(y)^{0.5}d_p(y)^{-0.5}. \tag{13}$$

If b and h are functions of y, flow velocity is related to flow rate by

$$u(y) = \frac{v_D}{b(y)h(y)} \tag{14}$$

and specific electrode surface of a pbe consisting of spherical particles can be written as

$$A_s = \frac{6(1-v)}{d_p(y)}. \tag{15}$$

Introducing Equations 13 and 14 into Equation 10, and rearranging leads to:

$$h(y) = \left(\frac{v\chi\Delta\eta\beta}{3(1-v)z_iFk'}\right)^{2/3} \times \left(\frac{v_D}{b(y)}\right)^{-1/3} d_p(y)c(y)^{-2/3}. \tag{16}$$

According to Equation 9, introduction of

$$i[\eta(x,y)] = k(y)c(y)zF, \tag{17}$$

and Equations 13 and 15 into Equation 6 results in

$$\frac{dc(y)}{dy} = -\left(\frac{6(1-v)k'}{d_p(y)^{3/2}u(y)^{1/2}}\right)c(y). \tag{18}$$

Equations 16 and 18 are the basic equations used in the following to establish the design equations for different kinds of pbe geometry.

3. Design equations [23, 24]

Volume flow rate, v_D, is calculated for the electrode entrance plane from Equations 14 and 16 by choosing values for three of the parameters $u(0)$, $b(0)$, and $d_p(0)$. At any further point y of the length coordinate of the pbe the values of $u(y)$, $b(y)$, $h(y)$ and $d_p(y)$ are related by Equations 14 and 16. Given two of these, the other two can be calculated from the properties of the waste water, the volume flow rate v_D, and the concentration $c(y)$. The variation of $c(y)$ is given by Equation 18.

The selection of values for $u(y)$, $b(y)$, $h(y)$ and $d_p(y)$, and which pair of them, is not only a question of electrochemistry, but also a question of ease of cell construction. So we consider three different design cases:

Case 1: Constant flow velocity $u(y) = u(0)$, and constant particle diameter $d_p(y) = d_p(0)$.

Case 2: Constant bed width $b(y) = b(0)$, and constant particle diameter $d(y) = d(0)$.

Case 3: Constant bed width $b(y) = b(0)$, and linear growing bed depth $h(y) = h(0) + \sigma y$.

These three cases are illustrated in Fig. 4. It may be interesting to apply different cases to different parts of one cell. For example, case 2 may lead to such an increase of $h(y)$ that it is impossible to construct a cell. So, from a certain point the design of the cell may be developed further as shown for case 3 in Fig. 5.

Each of the cases 1–3, together with the basic Equations 14, 16 and 18, gives a differential equation for $c(y)$. Inserting the solution of this differential equation into the basic equations yields the design equations.

The solutions of the differential equations give the dependence of the metal concentration on y and $c(0)$. For a given c_1 let y_1 be the length of the cell at which c_1 is achieved, i.e.

$$c_1 = c[y_1, c(0)].$$

We can give the solutions of the differential equations as functions of

$$y_1[c(0), c_1].$$

We do so in the following.

Case 1

Differential equation and solution†

† In the calculation, numerical values for the constants are used as given in Appendix 1. A derivation of the differential equations is given in Appendix 2.

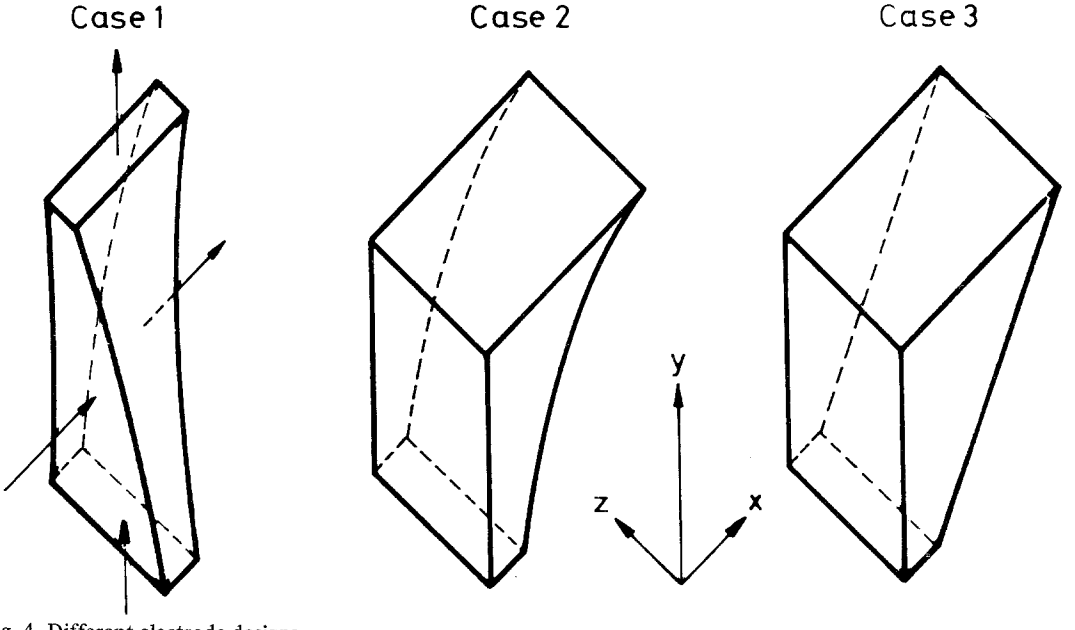

Fig. 4. Different electrode designs.

$$\frac{dc(y)}{dy} = -2.144 \times 10^{-3} \left(\frac{1}{d_p(0)^{3/2} u(0)^{1/2}} \right) c(y) \tag{19}$$

$$y_1 = \frac{10^3}{2.144} d_p(0)^{3/2} u(0)^{1/2} \ln \left(\frac{c_0}{c_1} \right). \tag{20}$$

Design equations

$$h(y) = 0.0736 d_p(0)^{3/4} \left(\frac{c_e^t}{\chi \Delta \eta} \right)^{-1/2} u(0)^{-1/4} \exp\left(1.072 \times 10^{-3} d_p(0)^{-3/2} u(0)^{-1/2} y\right) \tag{21}$$

$$b(y) = \frac{v_D}{u(0)h(y)}. \tag{22}$$

Case 2

Differential equation and solution:

$$\frac{dc(y)}{d(y)} = -2.144 \times 10^{-3} \times \left(\frac{1}{d_p(0)^{3/2} u(0)^{1/2}} \right) c(0)^{1/3} c(y)^{2/3} \tag{23}$$

$$y_1 = 1.40 \times 10^3 d_p(0)^{3/2} u(0)^{1/2} \left(1 - \frac{c_1}{c_0} \right)^{1/3}. \tag{24}$$

Design equations

$$h(y) = \left[5.695 \left(\frac{c_e^t}{\chi \Delta \eta} \right)^{1/3} d_p(0)^{-1/2} \left(\frac{v_D}{b(0)} \right)^{1/6} - 0.715 \times 10^{-3} d_p(0)^{-3/2} \left(\frac{v_D}{b(0)} \right)^{-1/2} y \right]^{-2} \tag{25}$$

$$u(y) = \frac{u(0)h(0)}{h(y)}. \tag{26}$$

Equation 25 implies that $h(y) \to \infty$ for y converging to a certain finite y_0. That is why it might be necessary to apply another design, beginning from a point $y < y_0$ as shown in Fig. 5.

Table 1.

Parameter	*Cell constructed according to case 1*		*Cell constructed according to case 2*	
	Prediction of the theory	*Experimental result*	*Prediction of the theory*	*Experimental result*
$v_D(l\,h^{-1})$	50	50	50	50
$\chi(S\,cm^{-1})$	0.019	0.019	0.001	0.001
c_0(ppm)	100	100	50	50
c_1(ppm)	1	0.13	0.1	0.02
I(A)	2.07	2.17	3.76	4.1
β(l)	0.60	0.57	0.56	0.51
U(V)	–	2.5	–	2.0

Case 3

Differential equation and solution:

$$\frac{dc(y)}{dy} = -2.144 \times 10^{-3} \left(\frac{1}{d_p(0)^{3/2} u(0)^{1/2}}\right) c(0) \left(\frac{h(0)}{h(0)+\sigma y}\right) \tag{27}$$

$$y_1 = \frac{h(0)}{\sigma} \exp\left[0.466 \times 10^3 d_p(0)^{3/2} u(0)^{1/2} \frac{\sigma}{h(0)} \frac{(c_0 - c_1)}{c_0}\right] - \frac{h(0)}{\sigma}. \tag{28}$$

Design equations

$$d_p(y) = 32.43[h(0)+\sigma y]u(0)^{1/3} \left(\frac{c_e^t}{\chi \Delta\eta}\right)^{2/3} h(0)^{1/3} \left[1 - 0.116 \times 10^{-4} \left(\frac{c_e^t}{\chi\Delta\eta}\right)^{-1} \frac{1}{u(0)h(0)^2} y\right]$$

$$\times \ln\left[\left(1 + \frac{\sigma y}{h(0)}\right) \frac{h(0)}{\sigma y}\right]^{2/3}. \tag{29}$$

For $\sigma \to 0$ this converges to:

$$d_p(y) = 32.43 h(0)^{4/3} u(0)^{1/3} \left(\frac{c_e^t}{\chi\Delta\eta}\right)^{2/3} \left[1 - 0.116 \times 10^{-4} \left(\frac{c_e^t}{\chi\Delta\eta}\right)^{-1} \frac{1}{u(0)h(0)^2} y\right]^{2/3} \tag{30}$$

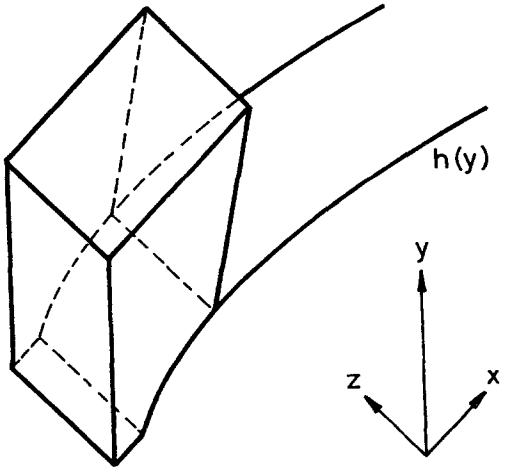

Fig. 5. Combination of two kinds of design principles in one electrode.

$$u(y) = \frac{u(0)h(0)}{h(0)+\sigma y} \tag{31}$$

Table 1 shows how reliably the theory predicts practical data.

In case 1, the metal to be recovered was silver and in case 2 the water was contaminated with Cu^{2+} ions. The experimental results are better than the theoretical prediction. An explanation may be that the particles of the packed bed are not exactly spherical and vary in shape and magnitude. So the real specific electrode surface is greater than that calculated.

4. Engineering aspects

In all cases the design of the cell depends very

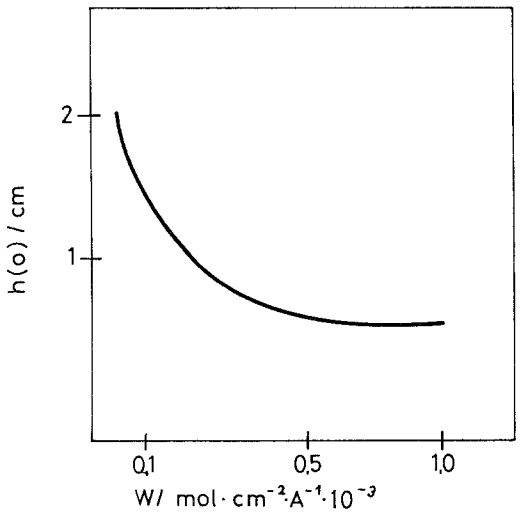

Fig. 6. Dependence of optimum bed depth on waste water parameter [$u(0) = 1$ cm s^{-1}, $d_p(0) = 0.125$ cm].

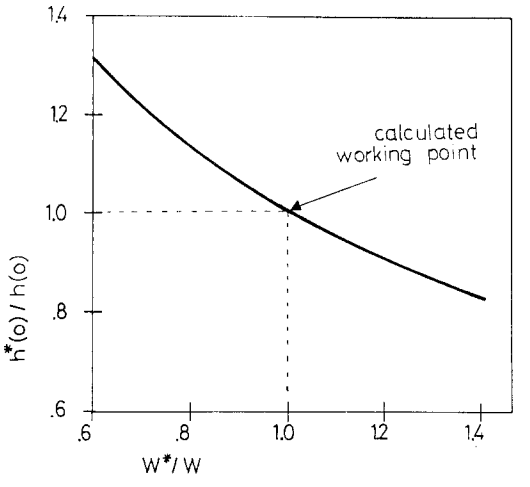

Fig. 7. Relative optimum bed depth as a function of the relative waste water parameter.

much on the quality of the waste water. Changing the total equivalent concentration of the electroactive species c_e^t or the conductivity requires a new design. This is a disadvantage, since:

(1) For construction it is more convenient to have a finite set of cells.

(2) Often, concentrations in waste waters are not constant with time. If the cell is designed for the worst case, it would not be optimal most of the time. This would imply a loss of volume flow rate of a cell unit.

(3) Clients ask for test runs and it is not efficient to construct a new cell for each test.

To overcome these difficulties one can adjust the cell to a variation in the waste water properties by changing operating parameters and the particle diameter in a given cell.

By 'cell profile' we mean a given cell with fixed width $b(y)$ and depth $h(y)$ as given in case 1, 2 or 3, but with $d_p(y)$ still to be chosen. For a given waste water, we choose $d_p(y)$ and $u(0)$ (or the corresponding v_D) in such a way that the design equations of the cell are fulfilled. So with a finite set of types, one can treat any waste water over a great range, as if the cell were constructed specially for a specific case. To overcome the variation of feed with time clearly this procedure is impossible. Here the solution will be to construct a loop as shown in Fig. 9. In Fig. 9 the conduit pipes are given by arrows and the instantaneous description of the system is given by the volume flow rates and the water parameters in each pipe. Cleaned water is 'recycled' in such an amount that the cell is working at optimum conditions at any moment.

In the design Equations 21, 25 and 29, the waste water data are always aggregated as

$$W = \frac{c_e^t}{\chi \Delta \eta}. \tag{32}$$

W is called the water parameter in the following. According to Equation 16, for a given $u(0)$ and $d_p(0)$, the optimal bed depth at the inlet, $h(0)$, is determined by W only. The dependence is given in Fig. 6. So in each of the three cases v_D is determined by W. For constant values of $b(0)$, $u(0)$ and $d_p(0)$, it follows from Equations 10 and 14 that

$$v_D \sim h(0) \sim \frac{1}{(c_e^t)^{1/2}}. \tag{33}$$

That is, the greater W, the lower the possible v_D and one can think of W as a kind of water contamination. If a cell fits for water with a parameter W_1 and $W_1 > W_2$, the cell is also suitable for W_2, since one can lower $\Delta\eta$.

The other parameters in the design equations are:

Parameters of the cell profile $h(y)$, $b(y)$.
Operation parameters v_D, or the corresponding $u(0)$.
$d_p(y)$, which one can regard as a variable construction parameter.

As can be seen from Equation 33 or from Fig. 6

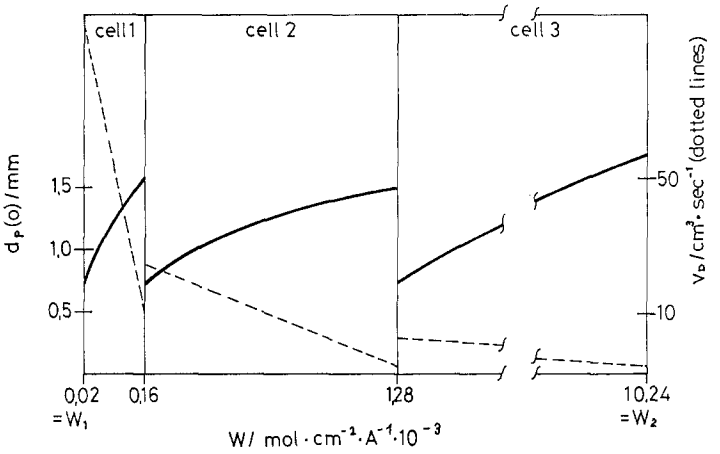

Fig. 8. Variation of d_p and v_D with waste water parameter W for three given cells of case 2 design.

the bed depth $h(0)$ is not very sensitive to changes in W. This is demonstrated again in Fig. 7, where a variation of ± 40 % of W is considered. To achieve a good degree of conversion with a cell, it is necessary for the bed depth to be less than or equal to $h(0)$, the bed depth which is calculated from the data W of the waste water. If $h(0)$ is too great, some of the water will pass through the cell without being cleaned (right side of Fig. 7).

For a given cell profile

$$h(y) = A \exp(By)$$

as determined by Equation 21 (case 1) and a given W the values of $d_p(y) = d_p(0)$ and $u(0)$ are calculated as follows: W, d_p and $u(0)$ should fulfill Equation 21. This implies that

$$A = 0.0736 d_p(0)^{3/4} W^{-1/2} u(0)^{-1/4} \quad (34)$$

and

$$B = 1.072 \times 10^{-3} d_p(0)^{-3/2} u(0)^{-1/2}. \quad (35)$$

This is equivalent to

$$d_p(0) = 0.583 A^{2/3} B^{-1/3} W^{1/3} \quad (36)$$

and

$$u(0) = 0.580 \times 10^{-5} A^{-2} B^{-1} W^{-1}. \quad (37)$$

Because $d_p \sim W^{1/3}$, a wide range of W can be covered by a small change in particle diameter.

For a given cell profile

$$h(y) = (A - By)^{-2}$$

as determined by Equation 25 (case 2) and a given W, the values of $d_p(y) = d_p(0)$ and v_D are calculated in a similar way. This yields

$$d_p(0) = 0.509 A^{-1} B^{-1/3} W^{1/3} \quad (38)$$

and

$$v_D = 0.387 \times 10^{-5} b(0) A^3 B^{-1} W^{-1}. \quad (39)$$

With these considerations, case 3 is the easiest of all, since given a cell profile

$$h(y) = h(0) + \sigma y$$

and

$$b(y) = b(0).$$

One chooses $d_p(y)$ with respect to Equation 29, whatever W may be.

It is interesting that for cases 1 and 2 the degree of conversion in a cell does not change if the cell is adapted to different values of W in the way just calculated. To see this, one considers Equations 20 and 24. For a fixed cell length y_1 the degree of conversion is given implicitly by these equations and only depends on the product $d_p(0)^{3/2} u(0)^{1/2}$. But it is just this product that remains constant if the cell is adapted to different values of W, as one can see, for example, for case 1 from Equation 35. For case 3, an adaption of a cell to different values of W does not change the degree of conversion if $d_p(0)^{3/2} u(0)^{1/2}$ remains constant. (This follows from Equation 28.)

An example is given in the following of how to calculate many of the different profiles needed for a given range of the water parameter W ($W_1 \leqslant W \leqslant W_2$):

For a water 1 with: $\chi = 0.16$ S cm^{-1}, 10 ppm dissolved oxygen and 15 ppm Hg^{2+}, one can make calculations for a water parameter of $W_1 \approx 0.000\,02$ mol cm^{-2} A^{-1} from Equation 32 ($\Delta\eta = 0.44$ V for Hg).

For a second water 2 with: $\chi = 0.001$ S cm^{-1}, 10 ppm dissolved oxygen and 50 ppm Cu^{2+}, one obtains $W_2 \approx 0.01$ mol cm^{-2} A^{-1} ($\Delta\eta \approx 0.28$ V for copper).

Therefore $W_2/W_1 = 500$.

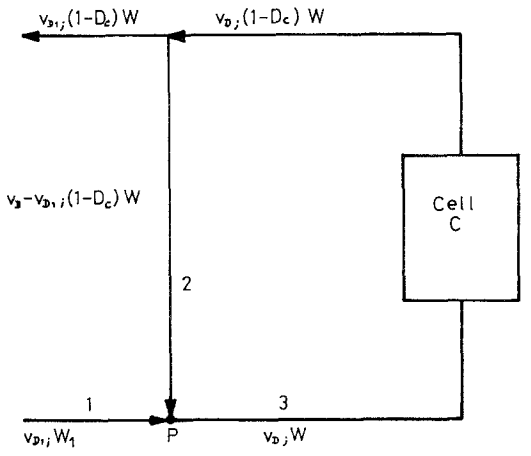

Fig. 9. Partial recycling of purified water to fit a cell to different W parameters.

If the particles available for the packed bed are in the range 0.75 to 1.5 mm in diameter, Equation 36 (or Equation 38) implies that one cell profile can be adapted to W differing by a factor of 8. Since

$$8^3 = 512 > \frac{W_2}{W_1} > 64 = 8^2$$

it is clear that three cell profiles are necessary and sufficient to cover the range W_1 to W_2 (see Fig. 8).

A maximum entrance flow velocity results from the demand of a certain final concentration and a reasonable limitation of reactor flow length (see Equations 20, 24, 28). A lower limitation of particle diameter is caused since one has to ensure a well-defined hydrodynamic flow and to avoid a particle agglomeration in the entrance and outlet regions. These conditions imply upper limitations of volume flow rate for a given cell profile:

From

$$v_D = u(y)b(y)h(y)$$

and

$$h(0) = A \exp(B \cdot 0) = A \qquad \text{(case 1)}$$

$$h(0) = [A - (B \cdot 0)]^{-2} = A^{-2} \qquad \text{(case 2)}$$

one gets

$$v_D \leqslant u(0)_{MAX} A\, b(0) \qquad \text{(case 1)}$$

$$v_D \leqslant u(0)_{MAX} A^{-2} b(0) \qquad \text{(case 2).}$$

On the other hand, the volume flow rate of case 1 (or case 2) cell can be calculated from Equations 36 and 37 (or Equations 38 and 39) as a function of A, B and $d_p(0)$.

$$v_D = \frac{1}{d_p(0)^3} f_i(A,B); \qquad i = 1,2$$

Therefore, the minimum particle diameter determines a second upper limit for v_D. If one wants to use the maximum $u(0)$ and the minimum d_p, then the two upper limits should be equal. The result is that A and B are not independent of each other.

Since the concentration of species in waste waters often varies with time, it may be useful to provide a possibility of adding a part of the cleaned water to the original waste water (see Fig. 9). A cell C constructed for purifying a volume flow rate v_D of water with parameter W has a certain conversion degree

$$D_C = \left(1 - \frac{c_1}{c_0}\right)$$

which is independent of the waste water, whenever its parameter is W or less (see the design equations). So the recycling operation mode only is necessary if $W_1 > W$.

Combining the two waste water streams at point P, a third stream is generated. With the assumption of constant conductivity its water parameter can be calculated from the mass balance of electroactive species at point P. The indices of c_e^t refer to the number at the conduit pipes (arrows) in Fig. 9:

$$c_{e3}^t v_D = c_{e1}^t v_{D1} + c_{e2}^t (v_D - v_{D1}). \qquad (40)$$

Since $\Delta\eta$ can be considered as constant, to a close approximation it follows that

$$W v_D = W_1 v_{D1} + (1 - D_C) W (v_D - v_{D1}). \qquad (41)$$

This is equivalent to

$$v_{D1} = v_D W \frac{D_C}{W_1 - (1 - D_C) W}. \qquad (42)$$

Equation 42 describes the dependence of the system volume flow rate v_{D1} for $W_1 > W$.

Example

For $D_C = 0.99$, $v_D = 200\,l\,h^{-1}$, $W = 0.01$ and $W_1 = 0.02$ one gets

$$v_{D1} \approx 99.5\,l\,h^{-1}.$$

According to the additional dilution effect of the

Table 2.

Element	c_0(ppm)	c_1(ppm)
Cu	20	0.07
Zn	8.6	0.12
Cd	22	0.61
Pd (parallel to Cu^{2+})	25	0.23
Hg (parallel to Fe^{3+}, Cl_2)	7.2	0.005

inlet stream it results in an improved overall degree of conversion of the system:

$$1 - \frac{(1 - D_C)W}{W_1} = 0.995 > D_C.$$

5. Technical applications

Table 2 gives the results achieved with a pilot plant (case 1 design) for different metals ($v_D = 50\,l\,h^{-1}$) [15]. Long-term experience with cells following case 2 design shows the technical applicability of the theory given here.

Appendix 1

Nomenclature and constants used in the calculations:

A_s	specific electrode surface (cm^{-1})
$b(y)$	width of the packed bed (cm)
$c(y)$	metal concentration (mol cm^{-3})
c_e^t	total equivalent concentration of electroactive species (mol cm^{-3})
D	diffusion coefficient ($cm^2\,s^{-1}$)
D_c	conversion degree (1)
$d_p(y)$	diameter of packed bed particles (cm)
F	Faraday number (96.487 As mol^{-1})
$h(y)$	bed depth parallel to current flow direction (cm)
$i(\eta)$	current density (A cm^{-2})
i_b	bed current density (A cm^{-2})
$i_g[c(y)]$	diffusion limited current density (A cm^{-2})
$\bar{i}$	mean current density of metal deposition (A cm^{-2})
$k(y)$	mass transfer coefficient (cm s^{-1})
k'	0.8121×10^{-3} cm $s^{-1/2}$
U	cell voltage (V)
$u(y)$	flow velocity (cm s^{-1})
v	voidage (0.56)
V_A	volume of anode compartement (cm^3)
V_B	volume of packed bed electrode (cm^3)
v_D	volume flow rate ($cm^3\,s^{-1}$)
W	water parameter (mol $cm^{-2}\,A^{-1}$)
x	coordinate parallel to current flow (cm)
y	coordinate parallel to electrolyte flow (cm)
y_{ST}^E	space time yield of the electrode (s^{-1} or $m^3\,h^{-1}\,l^{-1}$)
y_{ST}^C	space time yield of the cell (s^{-1} or $m^3\,h^{-1}\,l^{-1}$)
z	coordinate normal to current and electrolyte flow (cm)
z_i	charge number (1)
β	current efficiency (1)
η_1	overpotential near the feeder electrode (V)
η_2	overpotential near the membrane (V)
$\Delta\eta$	$\eta_2 - \eta_1$ (V)
$\eta(x,y)$	overpotential at point (x,y) (V)
ϕ_p	particle potential (V)
ϕ_s	electrolyte potential (V)
χ	electrolyte conductivity (S cm^{-1})
χ_p	particle conductivity (S cm^{-1})
χ_s	electrolyte conductivity (S cm^{-1})
ν	kinematic viscosity ($cm^2\,s^{-1}$)
σ	slope of the feeder electrode (1)

Appendix 2

Derivation of the differential equations.

Case 1

Replacing k' and v in Equation 18 by the values given above yields Equation 19.

Case 2

For case 2 one has:

$$\begin{aligned} b(y) &= b(0) \\ d_p(y) &= d_p(0). \end{aligned} \tag{A1}$$

Equation 14 implies

$$u(0)b(0)h(0) = u(y)b(y)h(y)$$

and together with Equation A1:

$$u(y) = u(0)\frac{h(0)}{h(y)}. \tag{A2}$$

Since

$$\beta = \frac{z_i c(0)}{c_e^t}$$

Equation 16 implies that:

$$h(y) = \left[\frac{v\chi\Delta\eta}{3(1-v)Fk'c_e^t}\right]^{2/3}\left[\frac{v_D}{b(y)}\right]^{-1/3} \times d_p(y)\left[\frac{c(0)}{c(y)}\right]^{2/3}. \tag{A3}$$

Together with Equation A1 this gives

$$\frac{h(0)}{h(y)} = \left[\frac{c(y)}{c(0)}\right]^{2/3}. \tag{A4}$$

Inserting this into Equation A2 yields

$$u(y) = u(0)\left[\frac{c(y)}{c(0)}\right]^{2/3} \tag{A5}$$

and this together with Equation 18 gives the differential Equation 23.

Case 3

The assumptions for case 3 are:

$$b(y) = b(0) \tag{A6}$$
$$h(y) = h(0) + \sigma y.$$

Together with Equation A3, this implies that

$$\frac{h(0)}{h(y)} = \frac{d_p(0)}{d_p(y)}\left[\frac{c(y)}{c(0)}\right]^{2/3}. \tag{A7}$$

Combined with Equation A6 and rearranging:

$$d_p(y) = \frac{d_p(0)\,[h(0)+\sigma y]}{h(0)}\left[\frac{c(y)}{c(0)}\right]^{2/3}. \tag{A8}$$

From Equation A2 it follows that

$$u(y) = u(0)\,\frac{h(0)}{[h(0)+\sigma y]}. \tag{A9}$$

Inserting Equations A8 and A9 into Equation 18 yields differential Equation 27.

Acknowledgement

The authors wish to acknowledge Bundesministerium für Forschung und Technologie for finanical support.

References

[1] D. N. Bennion and J. Newman, *J. Appl. Electrochem.* **2** (1972) 113.
[2] R. S. Wenger and D. N. Bennion, *J. Appl. Electrochem.* **6** (1976) 385.
[3] A. K. P. Chu, M. Fleischmann and G. J. Hills, *J. Appl. Electrochem.* **4** (1974) 323.
[4] A. T. Kuhn and R. W. Houghton, *J. Appl. Electrochem.* **4** (1974) 69.
[5] G. Kreysa, *Chem.-Ing.-Tech.* **50** (1978) 332.
[6] S. Germain and F. Goodridge, *Electrochim. Acta* **21** (1976) 545.
[7] F. Goodridge and C. J. Vance, *Electrochim. Acta* **22** (1977) 1073.
[8] H. Scharf, German patent DT 22 27 084 (1972).
[9] C. M. S. Raats, H. F. Boon and W. Eveleens, *Erzmetall.* **30** (1977) 365.
[10] G. v. Heiden, C. M. S. Raats and H. F. Boon, *Chem. Ind.* (1978) 465.
[11] P. M. Robertson, F. Schwager and N. Ibl, *J. Electroanal. Chem.* **65** (1975) 883.
[12] P. M. Robertson and N. Ibl, *J. Appl. Electrochem.* **7** (1977) 323.
[13] P. M. Robertson, B. Scholder, G. Theis and N. Ibl, *Chem. Ind.* (1978) 459.
[14] K. B. Keating and J. M. Williams, *Res. Rec. Cons.* **2** (1976) 39.
[15] P. Gallone, P. L. DeAnna and P. L. Bonora, *Mater. Chem.* **3** (1978) 285.
[16] D. Hutin and F. Coeuret, *J. Appl. Electrochem.* **7** (1977) 463.
[17] G. Kreysa, *Electrochim. Acta* **23** (1978) 1351.
[18] R. Alkire and P. N. Ng, *J. Electrochem. Soc.* **121** (1974) 95.
[19] D. J. Pickett, 'Electrochemical Reactor Design', Elsevier, Amsterdam, Oxford, New York (1977) p. 235 ff.
[20] M. Fleischmann and J. W. Oldfield, *J. Electroanal. Chem.* **29** (1971) 231.
[21] G. Kreysa, in preparation (1982).
[22] G. Kreysa and G. Leßmann, unpublished results (1976).
[23] G. Kreysa, German patent DOS 26 22 497.
[24] W. Dietz, H.-J. Reichenbach and C. Reynvaan, DOS 2904539.